

Supporting Information

Mesoporous MnFe₂O₄ magnetic nanoparticles as peroxidase mimic for colorimetric detection of urine glucose

Ke Liu[†], Jiaying Su[†], Jiangong Liang, Yuan Wu*

State Key Laboratory of Agricultural Microbiology, College of Science, Huazhong Agricultural University, Wuhan 430070, People's Republic of China

[†] These authors contribute equally to this work.

Corresponding Author:

Tel.: +86-2787288505

E-mail: yuanwu@mail.hzau.edu.cn (Yuan Wu)

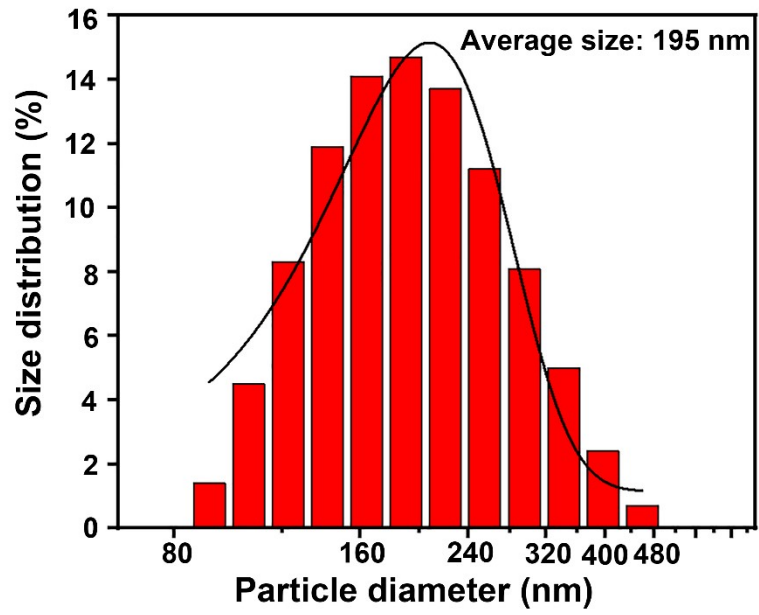


Fig. S1 Size distribution of DLS result for mMnFe₂O₄ MNPs.

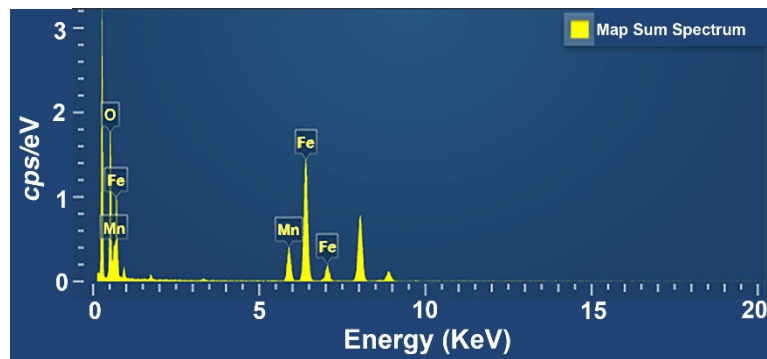


Fig. S2 EDS result for mMnFe₂O₄ MNPs.

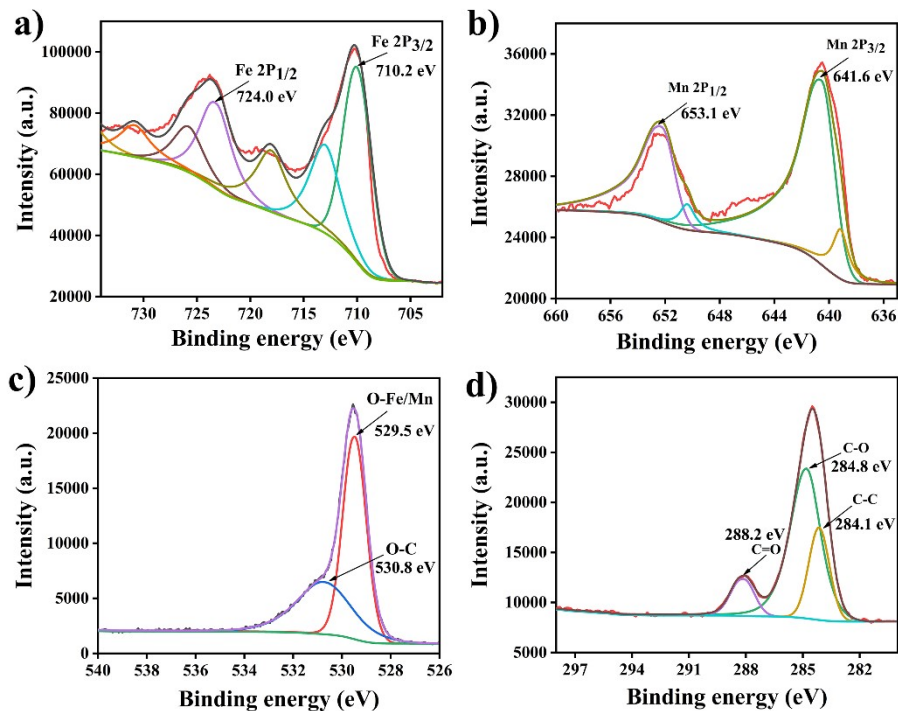


Fig. S3 XPS spectra of mMnFe₂O₄ MNPs: a) Fe 2p spectrum; b) Mn 2p spectrum; c) O 1s spectrum; d) C 1s spectrum. For the spectrum of Fe 2p, the peaks at 710.2 eV and 724.0 eV are attributed to Fe 2p_{3/2} and Fe 2p_{1/2}, respectively, indicating the presence of Fe³⁺. For the spectrum of Mn 2p (Fig. S4c), the peaks of Mn 2p_{3/2} and Mn 2p_{1/2} of binding energy are observed at 641.6 eV and 653.1 eV, indicating that Mn exists in the style of Mn²⁺. For the spectrum of O 1s (Fig.S4d), the peak at 529.8 eV relates to the oxygen in the form of O²⁻ in the nanocrystals. Form the fixed peak for the C 1s spectrum, the peaks at 288.2 eV, 284.8 eV and 284.1 eV are attributed to C 1s of C=O, C-O and C-C, which may be from organic molecules groups or CO₂ molecules.

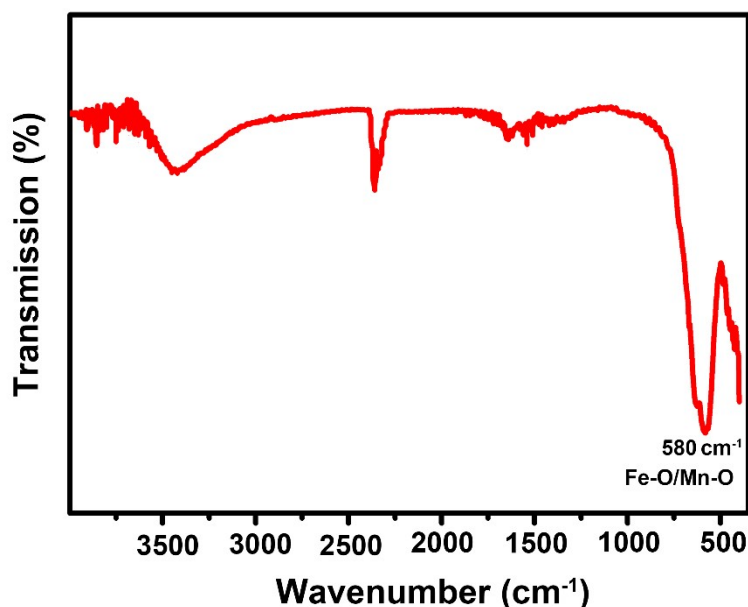


Fig. S4 FT-IR result of mMnFe₂O₄ MNPs. The strong band around 580 cm⁻¹ corresponds to the metal-oxygen stretching vibration bonds (Fe-O/Mn-O) in the nanomaterials.

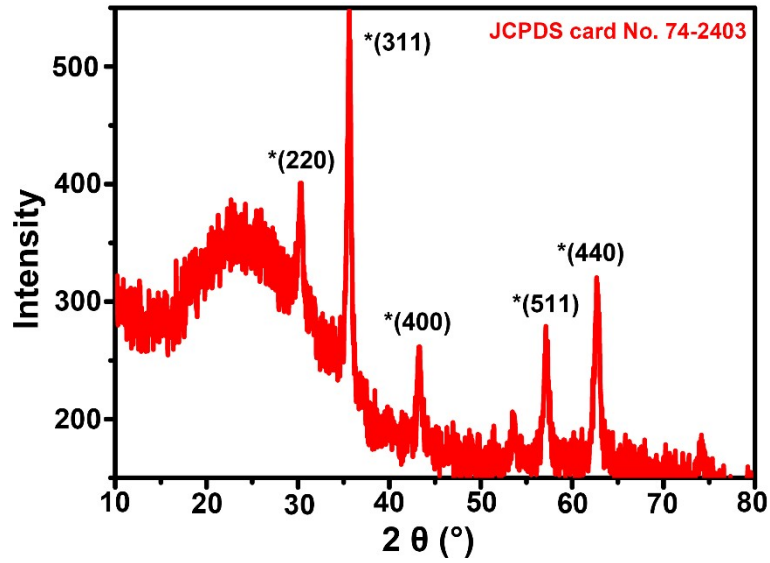


Fig. S5 XRD result for $m\text{MnFe}_2\text{O}_4$ MNPs.

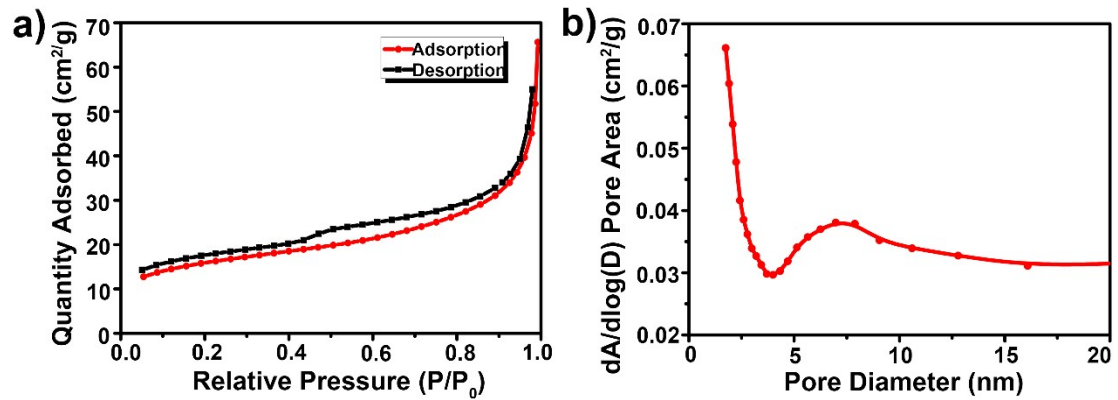


Fig. S6 a) N_2 adsorption-desorption result of $m\text{MnFe}_2\text{O}_4$ MNPs; b) HK pore size distribution curve of $m\text{MnFe}_2\text{O}_4$ MNPs.

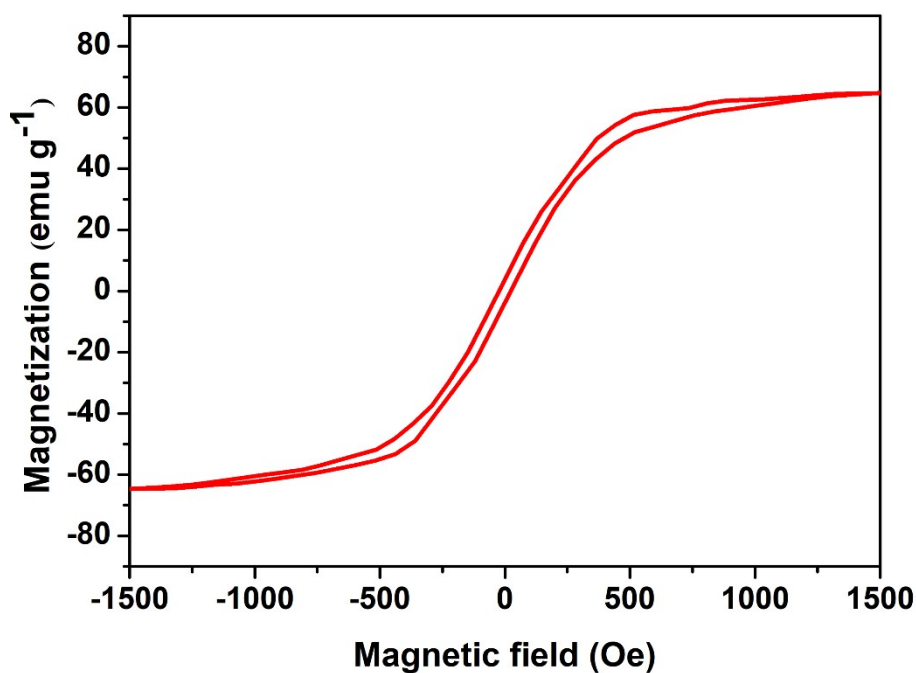


Fig. S7 Field dependent magnetization result of mMnFe₂O₄ MNPs.

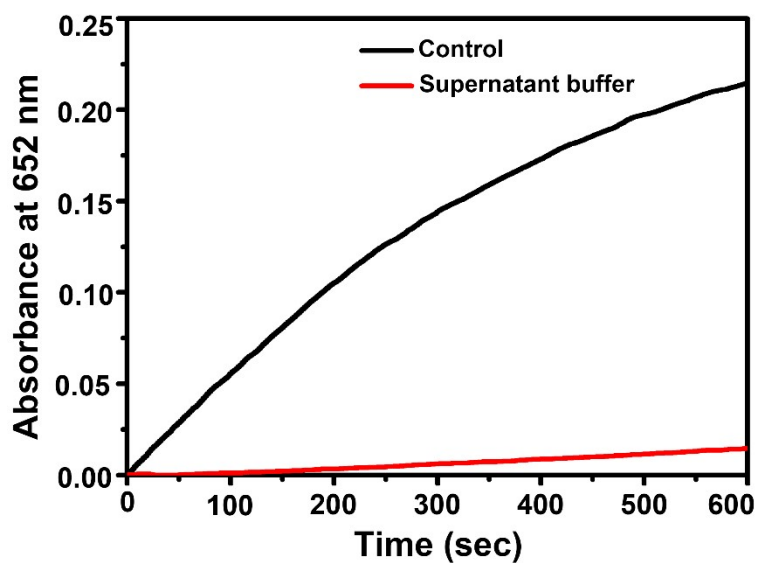


Fig. S8 Peroxidase-like activity of mMnFe₂O₄ MNPs (black line) and mMnFe₂O₄ MNPs incubated supernatant buffer (red line).

It is important to prove that the observed peroxidase-like activity was caused by mMnFe₂O₄ MNPs rather than leached ions from mMnFe₂O₄ MNPs in acidic solution. mMnFe₂O₄ MNPs were incubated in the reaction buffer (pH 4.0) for 2 h, and then catalytic assay was performed with supernatant solution by removing mMnFe₂O₄ MNPs with a magnet. As shown in Figure S8, no activity was observed with supernatant solution, confirming that the catalytic activity comes from the intact mMnFe₂O₄ MNPs.

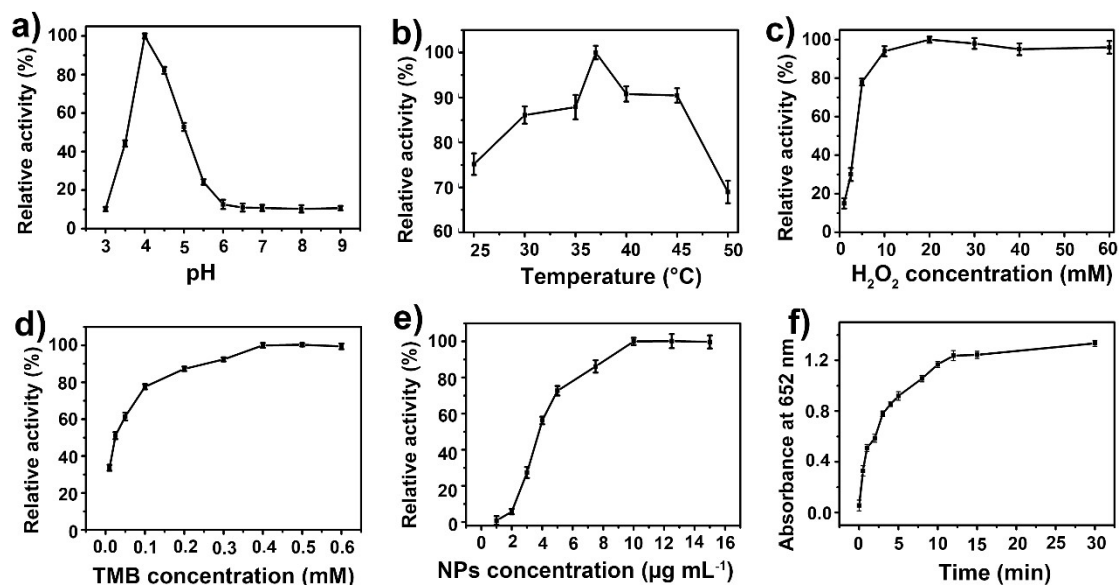


Fig. S9 Optimization of experimental parameters. a) pH optimization of mMnFe₂O₄ MNPs with TMB and H₂O₂ using absorbance at 652 nm; b) Incubation temperature optimization of mMnFe₂O₄ MNPs with TMB and H₂O₂ using absorbance at 652 nm; c) Optimization of H₂O₂ concentration; d) Optimization of TMB concentration; e) Optimization of mMnFe₂O₄ MNPs concentration; f) Reaction time optimization of mMnFe₂O₄ MNPs with TMB and H₂O₂ using absorbance at 652 nm.

The explanation for Fig. 3d:

To evidence the ·OH radical mechanism, fluorescence test of terephthalic acid (TA) were performed to detect ·OH during the catalytic reaction, since TA can react with ·OH to generate highly fluorescent 2-hydroxy terephthalic acid. Fig. 3d shows that the fluorescence intensity of TA at 435 nm significantly increased after adding mMnFe₂O₄ MNPs, whereas no fluorescence intensity was observed in the absence of H₂O₂ or mMnFe₂O₄ MNPs. These results demonstrate the catalytic mechanism of nanozymes is to bind and react with H₂O₂ and then release hydroxyl radical (·OH) to react with TMB.

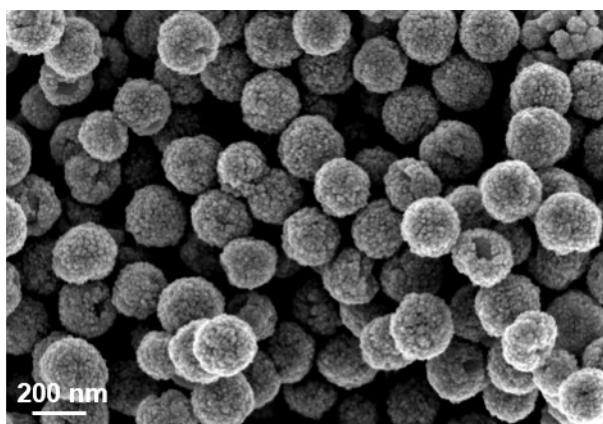


Fig. S10 SEM image of mMnFe₂O₄ MNPs kept in pH 4.0 for 2 h.

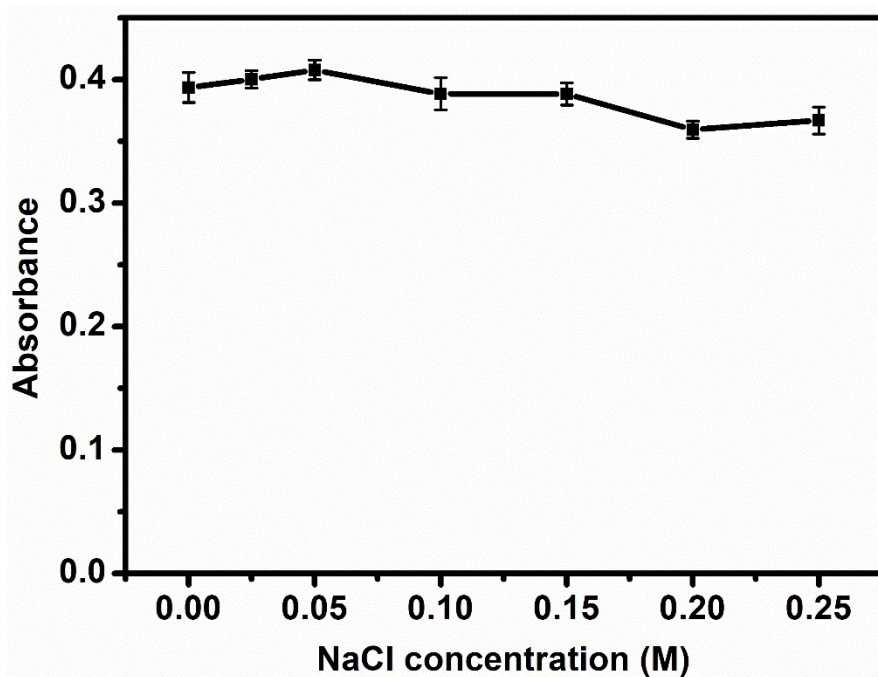


Fig. S11 Enzymatic-like reaction activity of $m\text{MnFe}_2\text{O}_4$ MNPs treated with different concentration of NaCl.

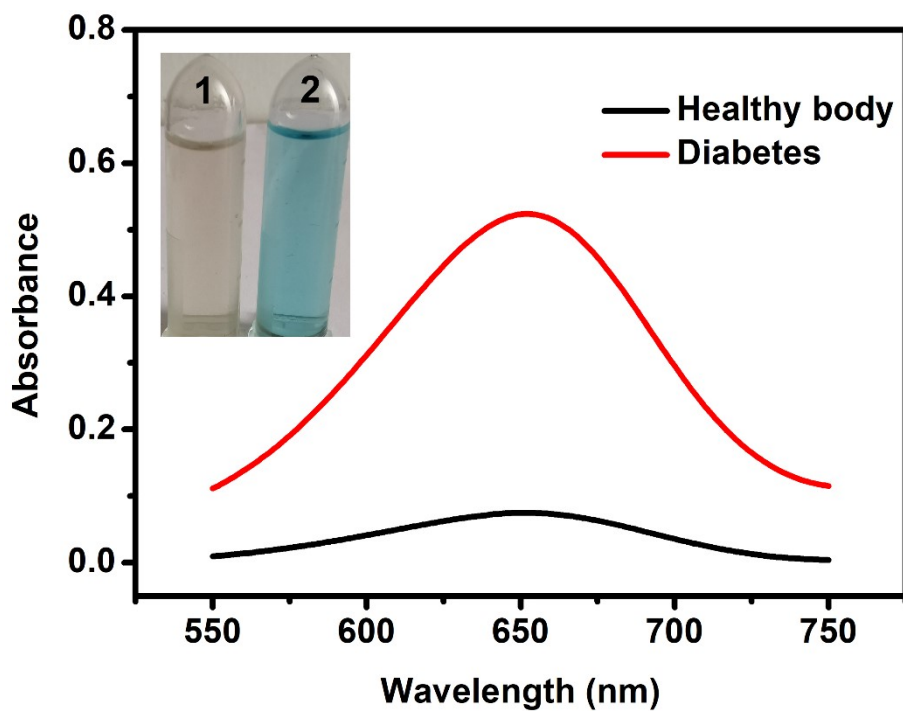


Fig. S12 UV-vis spectra of diluted urine samples from healthy body and diabetes. Inset: Images of colored production for urine samples. (1) healthy body and (2) diabetes.

Table S1. Comparison of the kinetic parameters^a of mMnFe₂O₄ MNPs nanozyme with other reported catalysts. TMB was the substrate.

Catalysts	K_m (mM ⁻¹)	V_{max} (10 ⁻⁸ M S ⁻¹)	Ref.
mMnFe ₂ O ₄ MNPs	0.07	27.8	This work
HRP	0.43	9.6	[1]
Hemin	0.75	6.2	[2]
Fe ₃ O ₄ MNPs	0.10	3.4	[1]
MoS ₂ /GO	0.10	33.4	[3]
FePt	0.121	21.1	[4]
ZnFe ₂ O ₄	0.85	13.3	[5]
Co ₃ O ₄	0.037	6.27	[6]
PtPd-Fe ₃ O ₄	0.079	9.36	[7]

^a The concentration of mMnFe₂O₄ MNPs was 10 µg mL⁻¹, H₂O₂ concentration was 20 mM.

Table S2. Comparison of other nanozyme probes for glucose analysis.

Nanozyme probes	Linear range	LOD	Ref.
mMnFe ₂ O ₄ MNPs	0.5-16 µM	0.7 µM	This work
Fe ₃ O ₄ MNPs	50-1000 µM	30 µM	[8]
Wse ₂ nanosheets	10-60 µM	10 µM	[9]
Cu _{0.89} Zn _{0.11} O	25-500 µM	1.5 µM	[10]
Nanosized CuS	0.5-110 µM	0.13 µM	[11]
SO ₄ ²⁻ /CoFe ₂ O ₄	0-300 µM	6.4 µM	[12]
CoFe ₂ O ₄	0.1-10 µM	0.024 µM	[13]
ZnFe ₂ O ₄	1.25-18.75 µM	0.3 µM	[5]
ZnO-ZnFe ₂ O ₄	1-23 µM	0.4 µM	[14]

Table S3 Determination of glucose in urine from health body (n = 3) with the mMnFe₂O₄ MNPs nanozyme probes.

Added (μM)	Total found (μM)	Recovery (%) n = 3	RSD (%) n = 3
1	0.93	93.4	4.5
10	10.65	106.5	7.4

References

- [1] L. Z. Gao, J. Zhuang, L. Nie, J. B. Zhang, Y. Zhang, N. Gu, T. H. Wang, J. Feng, D. L. Yang, S. Perrett, and X. Y. Yan, *Nat. Nanotechnol.*, 2007, **2**, 577-583.
- [2] X. C. Lv and J. Weng, *Sci. Rep.*, 2013, **3**, 3285-3294.
- [3] J. Peng and J. Weng, *Biosens. Bioelectron.*, 2017, **89**, 652–658.
- [4] Y. Liu, D. L. Purich, C. C. Wu, Y. Wu, T. Chen, C. Cui, L. Q. Zhang, S. Cansiz, W. J. Hou, Y. Y. Wang, S. Y. Yang, and W. H. Tan, *J. Am. Chem. Soc.*, 2015, **137**, 14952-14958.
- [5] L. Su, J. Feng, X. M. Zhou, C. L. Ren, H. H. Li, and X. G. Chen, *Anal. Chem.*, 2012, **84**, 5753-5758.
- [6] J. Mu, Y. Wang, M. Zhao, L. Zhang, *Chem. Commun.*, 2012, **48**, 2540–2542.
- [7] X. L. Sun, S. J. Guo, C. S. Chung, W. L. Zhu, and S. H. Sun, *Adv. Mater.*, 2013, **25**, 132–136.
- [8] H. Wei, and E.K. Wang, *Anal. Chem.*, 2008, **80**, 2250-2254.
- [9] T.M. Chen, X.J. Wu, J.X. Wang, and G.W. Yang, *Nanoscale*, 2017, **9**, 11806-11813.
- [10] A.P. Nagvenkar and A. Gedanken, *ACS Appl. Mater. Interfaces*, 2016, **8**, 22301-22308.
- [11] X. H. Niu, Y. F. He, J. M. Pan, X. Li, F. X. Qiu, Y. S. Yan, L. B. Shi, H. L. Zhao, and M. B. Lan, *Anal. Chim. Acta*, 2016, **947**, 42-49.
- [12] X. L. Yin, P. Liu, X. C. Xu, J. M. Pan, X. Li, X. H. Niu, *Sens. Actuator B Chem.*, 2021, **328**, 129033-123041.
- [13] W. B. Shi, X. D. Zhang, S. H. He, and Y. M. Huang, *Chem. Commun.*, 2011, **47**, 10785-10787.
- [14] M. G. Zhao, J. Y. Huang, Y. Zhou, X. H. Pan, H. P. He, Z. Z. Ye, and X. Q. Pan, *Chem. Commun.*, 2013, **49**, 7656–7658.